Recent Metal Fuel Safety Tests in TREAT*

A. E. Wright, T. H. Bauer, R. K. Lo, W. R. Robinson, and R. G. Palm

CONF-860501--9

DE86 012125

Argonne National Laboratory
9700 South Cass Avenue
Argonne, IL 60439 USA

* Work performed under the auspices of the US Department of Energy.

Work supported by the U.S. Department of Energy, "Technology Support Program" under Contract W-31-109-Eng-38.

In-reactor safety tests have been performed on metal-alloy reactor fuel to study its response to transient-overpower conditions, in particular, the margin to cladding breach and the axial self-extrusion of fuel within intact cladding. Uranium-fissium EBR-II driver fuel elements of several burnups were tested, some to cladding breach and others to incipient breach. Transient fuel motions were monitored, and time and location of breach were measured. The test results and computations of fuel extrusion and cladding failure in metal-alloy fuel are described.

INTRODUCTION

1. A series of tests is being conducted in the Transient Reactor Test (TREAT) Facility to provide basic empirical information on the transient behavior of metal-alloy fast reactor fuel under accident conditions. The near-prototypic test environment that can be created in-pile is being used to confirm inherent safety-related features of the fuel and to provide guidance to safety modeling and analysis of fuel behavior for the Integral Fast Reactor (IFR) concept. Many TREAT tests have been performed on metal fuel during the 1960's. However, the subsequent advances in metal fuel design that allow for higher swelling, higher burnup, and greater margin to failure dominate the analysis of the fuel element's response to off-normal conditions, thereby making much of the older in-pile database obsolete. New tests were needed to provide critical information for making safety assessments of the IFR conceptual design.

2. The objectives of the tests were to obtain information on two key fuel behavior characteristics under transient overpower (TOP) conditions in metal-fueled fast reactors: the margin to cladding breach and the axial self-extrusion of fuel within intact cladding. Cladding breach depends upon (a) penetration of the cladding wall by formation of a low-melting-point fuel-steel alloy and (b) the internal pin pressure. Driving forces for fuel extrusion are fission gas, liquid bond sodium, and volatile fission products trapped within the fuel. Significant fuel extrusion prior to cladding breach would be an important factor in the case for benign termination of unprotected overpower events in a fast reactor.

3. Four TOP tests have been performed on uranium- 5% fission EBR-II Mark-II driver fuel pins. These pins were suitable and available stand-ins for the U-Pu-Zr ternary alloy chosen as the reference IFR fuel. A preliminary test (M1) optically studied open-ended segments of an irradiated fuel element without sodium coolant to determine whether extensive solid-fuel extrusion occurs. In this test, as in the three loop tests described below, it appears that appreciable extrusion occurred only after the fuel melted.

4. In tests M2, M3, and M4, intact irradiated pins were tested in TREAT Mark-III flowing sodium loops. In each test three pins were included, each in a separate, orificed flowtube. The experiments included pins of low, medium, and high burnup. In all three tests, the power rose exponentially from near

nominal on an 8 s period. During the power rise, the thermal performance of each pin was monitored by nearby thermocouples, and axial extrusion was measured by the TREAT fast neutron hodoscope. It was intended that some of the pins would be heated to incipient cladding breach, whereas others would be heated slightly beyond. Cladding failure events were monitored by thermocouples, pressure transducers, flowmeters, and the hodoscope. The power transients were rapidly terminated upon cladding breach. Results of the loop tests and associated analyses are described below.

MARGIN TO CLADDING FAILURE

5. The nine pins tested in the three loop tests included pins of five burnup levels, including zero burnup. Three of the pins, of 2.4 at.%, 4.4 at.%, and 7.9 at.% burnup, were heated to cladding breach. According to the "pressure assisted meltthrough model" described in a following paragraph, the temperatures that control cladding failure, i.e., the gas-plenum, peak mid-cladding, and peak fuel-cladding-interface temperatures, are all principally functions of the whole-pin power-to-flow (P/F) ratio. Thus, when expressed in terms of the P/F ratio, the cladding failure threshold measured in the tests are not only directly comparable with each other but also directly applicable to margin-to-failure assessment of pins operating in a fast reactor.

Observed margin to failure

6. Table 1 shows the peak values of the P/F ratio achieved for each of the pins tested. Values of the P/F ratio are normalized to the value at IFR normal operating conditions. Computed values of the gas pressure in the pin plenum at peak P/F are also indicated. The P/F values at observed cladding failure (4.1 to 4.2) are all essentially the same despite the wide range of plenum pressure (as low as 2 MPa for 2.4 at.% burnup, extending up to 20 MPa for 7.9 at.% burnup). This is probably a consequence of a temperature threshold for rapid cladding attack by eutectic formation, described below. In these tests, cladding failures occurred only at the top of the fuel, as predicted, since in slow transients, mid-clad and fuel- cladding interface temperatures peak there. Dimples fabricated in the cladding just above the top of the active fuel may have played a role in cladding failure.

Computed margin to failure

7. SAS4A (Ref. 1) and COBRA (Ref. 2) computer codes were modified to include a pressure-assisted meltthrough model for cladding failure in sodium-bonded metal fuel. Melting below the steel melting point by fuel-steel alloy formation is assumed. Calculations assume that the fuel is structurally weak and cladding is under only hydrostatic loading from a time-dependent plenum pressure. Cladding stresses reflect not only the pin plenum pressure but also thinning by penetration of low temperature eutectic. Time-to-failure is estimated from plastic strain to rupture correlations. Current analyses use a simple correlation for penetration rate that depends only on the temperature of the fuel cladding interface. At all but the highest burnups, failure would not be expected until the fuel-cladding interface temperature exceeds a temperature above which eutectic penetration into the cladding becomes very rapid. Out-of-pile measurements indicate that this "critical" temperature is about 1350 K. Under steady-state conditions, rapid meltthrough would occur at a P/F ratio of about four. The failures observed in the 2.4 at.% and 4.4 at.% burnup pins occurred at P/F ratios slightly higher than this value, in good agreement with this concept. Failure of pins of very low burnup is predicted by the model only after the cladding is nearly completely penetrated by eutectic formation. On the other hand, the peak plenum pressure in the 7.9 at.% burnup pins was so high that failure was computed to occur before significant thinning of the cladding took place.

8. Results of the cladding failure computation using the pressure-assisted meltthrough model are given in Table 1 in terms of P/F at failure. The range in value for the 7.9 at.% burnup pins arises from the uncertainty in the room-temperature plenum pressure. Considering the ~5% uncertainty in measured test fuel powers and flow rates (or P/F values from coolant temperature rises), and recognizing that potentially-significant test-fuel power changes due to pre-failure fuel motion were not taken into account, the agreement with the observed behavior seems satisfactory.

9. The proximity to cladding failure is indicated in the table in terms of deviation of the peak P/F value achieved in the test relative to the P/F value measured at cladding breach in pins of 4.4 and 7.9 at.% burnup, or relative to the P/F value at computed breach conditions for pins of 0, 0.35 and 2.4 at.% burnup.

PREFAILURE FUEL ELONGATION

Observed expansion

10. Transient fuel motion was monitored by the TREAT fast-neutron hodoscope. A cursory analysis of the data has been made for all three tests. Figure 1 shows representative measured prefailure elongation of this U-5Fs fuel at the several burnups tested. A curve for the fresh fuel is not shown because its expansion (1%) was so slight. An error bar indicates the approximate magnitude of the statistical uncertainty in the measurements. Systematic error could be significantly larger. The last three columns of Table 1 show the P/F values at the computed onset of fuel melting, the P/F values when half the total measured elongation was reached, and the total measured fuel elongation.

11. Total pre-failure elongation was more than 17% (relative to the pretest fuel length) in the 0.35 at.% burnup fuel. Fuel of 2.4 at.% burnup elongated about 7%. At 4.4 and 7.9 at.% burnup, the total elongation was only about 4%. Axial expansion of the magnitude observed (~ 10%) would imply a large negative reactivity effect in a reactor such as the IFR concept. Corresponding behavior of the U-Pu-Zr alloy selected as the reference IFR fuel will be measured in test M5 and subsequent tests.

Mechanisms for expansion

12. Modeling of extrusion look principally toward expansion of dissolved fission gas as the driving mechanism. However, boiling of the sodium bond is also a possibility when the pin plenum pressure is sufficiently low and the bond sodium is trapped within the fuel. Theoretical considerations as well as test results indicate that, for overpower transients of interest, extrusion significantly beyond thermal expansion does not occur until melting.

13. Fuel expansion in the solid state is believed to be very limited for two reasons. The first is that bubble coalescence is not a likely event, and surface tension in small bubbles severely limits the equilibrium values of individual bubble expansion. The second is that both direct measurement and theoretical argument now support the notion that most fission gas retained in the fuel is located in the coldest regions of the fuel pin, where it does not significantly contribute to fuel expansion. Analysis of recent gas retention data leads one to anticipate that in the hotter regions of the fuel the

retained gas concentration is only about the amount generated in 0.5 at.% burnup (Ref. 3). This is about one fourth of the whole-pin average gas retention at burnups greater than 2 at.%. Prior to melting, on the basis of single bubble expansion to equilibrium, this amount of dissolved gas could produce a net axial expansion of 1% or less (depending upon the pin plenum pressure) beyond normal thermal expansion which is itself of order 1%.

14. After extensive fuel melting takes place, circumstances become favorable for fuel expansion. Bubble expansion to equilibrium is rapid, and coalescence of small fission gas bubbles is sufficiently probable that surface tension no longer constrains the expansion. The amount of axial extrusion is effected principally by allowing the volume of all fission gas dissolved in molten fuel to expand to the pressure of the pin plenum. Under these circumstances, calculations of axial expansion needs very little "mechanical dynamics" and requires only a thermal analysis to determine the amount of molten fuel (to quantify available, dissolved fission gas) and to determine the temperatures of both molten fuel and pin plenum (to calculate fuel expansion at pressure balance).

15. Qualitatively, neglecting bubble surface tension is supported by test data that indicate peak axial expansions are very sensitive to pin plenum pressure, even at low burnups. Moreover, after test power shutdown, the expansions observed appear largely permanent, as is also consistent with expansion brought on by bubble coalescence. Quantitatively, without the considerable constraint of surface tension and with about half the fuel molten (a condition likely just prior to cladding failure), even the low level of gas concentration assumed above could lead to axial expansions as high as 20% in low burnup fuel, falling off rapidly as fuel burnup increases, down to about 2% for fuel of 8 at.% burnup.

Model for computing expansion

16. Calculations were performed using the COBRA-EXP code, which includes an added capability of computing the time-dependent axial expansion based on the assumptions noted above. The model for the expansion is simple. Fission gas within the fuel that causes fuel expansion is assumed to initially be dissolved in the fuel and to have negligible volume. Upon fuel melting, the dissolved gas is assumed to immediately form bubbles of zero surface tension and come into pressure equilibrium with the fuel-pin plenum gas. The plenum

pressure arises from (a) known amount of fission gas release from the fuel during preirradiation to its present burnup, (b) heating of the plenum by the sodium during the test, and (c) reduction of the plenum volume by the fuel expansion during the test. Ideal gas behavior is assumed. Thus, the post-equilibration fuel volume, i.e., the fuel expansion beyond normal thermal expansion, is given by

$$\Delta V_f = n_f R T_f / p_{eq}$$

where n_f is the quantity of gas in the molten fuel, T is its temperature, R is the gas constant, and p_{eq} is the equilibrium pressure (equal to the plenum pressure). The initial plenum volume $V_{p,o}$ is decreased by ΔV_f. Expressing p_{eq} in terms of the temperature T_p and gas content n_p of the plenum leads to the result

$$\frac{\Delta V_f}{V_{f,o}} = \frac{V_{p,o}}{V_{f,o}} \left(1 + \frac{n_p T_p}{N_f T_f} \right)^{-1}$$

where $V_{f,o}$ is the initial fuel volume in the pin.

17. To illustrate the overall extrusion behavior versus burnup that the model predicts, a simplified situation may be assumed in which the following conditions pertain at maximum expansion: 40% molten fuel, average molten-fuel temperature equal to the fuel liquidus temperature, and outlet sodium temperature corresponding to a fuel power of four times nominal. These conditions are typical of these computed by COBRA-EXP for all test pins.

18. Figure 2 presents for comparison the expansions computed by COBRA-EXP with the measured expansions for the fuel pins tested. The dashed curve pertains to the assumed illustrative situation described in the preceding paragraph and shows the general trend of the computation at low burnups. The cusp at 0.5 at.% burnup is, of course, the result of the assumed onset of fission gas release from the fuel when reaching that burnup during steady-state irradiation. As shown by Figure 2, the model appears to describe well the general expansion behavior of the U-5Fs fuel. The magnitude of the expansion also seems to be reasonably-well predicted, considering the uncertainty in the measurements and in the calculation of the fuel-coolant thermal-hydraulics. The latter includes uncertainty in the thermal conductivity of medium-to-high burnup fuel, which has a 25% pore fraction, part of which could be logged with high conductivity sodium.

19. Key modeling assumptions that could also influence extrusion timing include fission gas distribution and bubble coalescence. The distribution of dissolved gas could be skewed and become available at powers other than expected with the assumed uniform distribution. The presumed coalescence of small bubbles may not be instantaneous after melting but involve some time delay. These questions will require more sophisticated analysis and modeling to resolve.

Applicability of the expansion measurements

20. It has been assumed in the modeling that significant expansion (beyond thermal expansion) only occurs when fuel melts into a gas-containing region. The timing and magnitude of extrusion therefore depends strongly on both the distribution of fission gas within the fuel as well as the transient temperature distribution within the fuel. In the thermal neutron flux in TREAT, the radial distribution of fission power generated in the test fuel is strongly peaked near the outer radius. This leads to a flatter radial temperature profile than prototypic. In test M4, this deficiency was overcome by scaling both the test-fuel power and the sodium flowrate upwards by about 25% relative to nominal. (The correct P/F ratio was maintained by this method, but slight adjustment of the inlet sodium temperature was necessary to compensate for the effect of these changes on peak cladding temperatures.) The solidus profiles shown in Figure 3 illustrate the effect of this compensation. The curves apply to a 4.4 at.%-burnup pin at a P/F value corresponding to about half-maximum fuel expansion. The compensation for test M4 resulted in a melt profile close to the prototypic ("reference") profile, a substantial improvement over the uncompensated situation in tests M2 and M3. The onset and magnitude of fission-gas-driven axial fuel expansion observed in test M4 should thus be more prototypic than that observed in tests M2 and M3.

21. The improved temperature profile, with its higher peak temperatures, should tend to cause an earlier onset of expansion and a greater magnitude of expansion. This is consistent with the early rise in the elongation curve shown in Figure 1 for the 2.4 at.% burnup fuel. The only other preirradiated fuel in test M4 was of 4.4 at.% burnup. Hodoscope data for that fuel pin were not as good as for the 4.4 at.% burnup pin of test M3 but do appear to indicate very rapid expansion at P/F=3.2 to a plateau of ~4% expansion. It is planned to use this technique of improving the radial temperature profile in up-coming tests on U-Pu-Zr fuel, as well.

POSTFAILURE FUEL MOTION

22. In the tests, fuel pins of 2.4 at.%, 4.4 at.%, and 7.9 at.% burnup failed. Post-failure fuel motion was monitored by the fast-neutron hodoscope. The final fuel distribution was recorded in posttest hodoscope scans and neutron radiographs. Although only very weak coolant pressure events occurred upon cladding failure, they were sufficient to rapidly reduce the inlet flow rate. Such reduction was anticipated, and its occurrence was set up to trigger a rapid (0.2-second) reactor-power shutdown. This plan successfully prevented severe destruction of the failed pins, prevented undesired additional pin failures, and essentially preserved the condition of the unfailed fuel pins that pertained at peak power.

23. All three pins failed near the top of the active fuel column, where the cladding was hottest and, therefore, where failure was expected. The fabricated "dimples" in the cladding (crimps in the cladding to prevent upward fuel relocation during preirradiation handling) at that location may have been the failure site, but it is unknown whether they caused failure to occur prematurely. Massive fuel ejection occurred in all three failed pins, with the fuel being ejected only through the very localized breach. Nearly all of the ejected fuel monotonically dispersed upward beyond the initial fuel zone. In the 2.4 at.% burnup pin, the ejected fuel originated from the upper 3/4 of the fuel column. More than half of the fuel initially in the top half of the fuel column left the cladding, and below the midplane there was significant density reduction. Within the 4.4 at.% burnup pin, voiding began in the lower 2/3 of the original fuel zone, and when fuel motion stopped, the bottom half of the fuel column had less than half of its initial amount of fuel. Within the 7.9 at.% burnup pin, fuel voiding began along the top half of the fuel column. Voiding subsequently moved to the bottom quarter, and, when fuel motion stopped, the bottom half of the fuel column was about 90% voided. A likely cause of the rapid fuel dispersal upon cladding failure is sudden flashing of sodium, logged within the fuel porosity, as the pin rapidly depressurizes. The greater disruption in the high burnup pin correlates with the greater depressurization.

24. The stainless steel flowtubes were 0.37 mm thick, similar to the cladding thickness. Despite the extensive postfailure fuel motion within the coolant channels and the fact that flowtube temperatures locally exceeded

1350 K for about one second, the flowtube walls containing the molten fuel and fuel-steel alloy from the failed pins were not completely penetrated by eutectic formation.

25. As indicated in Table 1, at peak power the fresh fuel in test M4 had expanded an amount equal to normal thermal expansion. The posttest hodoscope scan and neutron radiography shows that the top of the fuel column had slumped downward about 2.5 cm (7% of the initial fuel length) and radially outward to the cladding. That motion apparently occurred during power shutdown. This behavior is in contrast to that of the preirradiated fuel, in which the expansion that occurred during the test was preserved during shutdown.

POSTTEST EXAMINATIONS

26. Examinations are underway of the remains of the failed pins, the unfailed pins, and untested irradiated sibling pins. Thus far, the intact tested and untested pins have been nondestructively examined, and the failed pins have been studied metallographically. The presence of a single failure site, located at the top of the active fuel column, was confirmed. Fuel-steel eutectic attack of both the inside and outside of the cladding was studied optically and with scanning electron microscopy. Examination of the unfailed pins is expected to provide valuable information regarding cladding attack, axial fuel density distribution, and changes in the morphology and distribution of fuel porosity resulting from the test.

CONCLUSIONS

27. The results of these tests have both aided in the development of and validated the fuel extrusion and pin cladding failure models developed for analysis of metallic fuel within reasonable uncertainties, for uranium-fissium alloy. Data from the posttest examination of both failed and nearly-failed pins, and refinements of the present fuel performance models, will lead to more comprehensive understanding of metal fuel phenomena and provide direction for study of the U-Pu-Zr IFR reference fuel alloy both in and out of pile.

ACKNOWLEDGMENTS

R. H. Sevy, who provided many useful insights in this work, and G. S. Stanford, E. A. Rhodes, and R. C. Doerner, who analyzed and interpreted the hodoscope data, are respectfully acknowledged.

REFERENCES

1. WIDER, H. U., et al. Status and Validation of the SAS4A Accident Analysis Code System. Proceedings of the LMFBR Safety Topical Meeting, Lyon, France, July 1982, vol. II, 13-23.

2. FROEHLE, P. H and BAUER, T. H. COBRA-PI: An Extension of the COBRA-3M Code Dynamically Dimensioned to Accept Pin Bundles of Any Size. Proceedings of the American Nuclear Society Mathematics and Computations Division Topical Meeting, March 1983, 211.

3. SEVY, R. H., Argonne National Laboratory, personal communication, December 1985.

Table 1. Measured and Computed Values Pertaining to Cladding Failure and Prefailure Fuel Expansion

Test	Fuel Burnup (at.%)	Max. P/F Achieved in Test	Computed Peak Plenum Pressure[a] (MPa)	P/F at Computed Failure	Proximity to Failure (%)	Computed P/F at Onset of Fuel Melting	P/F at Half of Max. Fuel Elongation	Maximum Fuel Elongation (%)
M2	0.35	4.1	0.6-0.8	4.7	13	3.5	3.6	16
	4.4	4.2 (f)	7-9	4.5	(f)	2.7	3.8	(c)
	7.9	4.1 (f)	17-20	3.6-4.0[b]	(f)	2.7	2.9	3
M3	0.35	4.1	0.6-0.8	4.8	15	3.5	3.7	18
	4.4	4.0	7-9	4.4	5	2.5	3.1	4
	7.9	3.4	17-23	3.6-4.0[b]	17	2.5	2.5	4
M4	0.0	3.8	0.6-0.8	4.3	12	3.3	--	1
	2.4	4.1 (f)	2-6	4.4	(f)	2.3	3.2	8
	4.4	3.8	7-9	4.1	10	2.1	3.2	4

(a) The range shown reflects the uncertainty in the room-temperature pressure.
(b) Reflects the range in computed plenum pressure at failure.
(c) Data are very ambiguous but seem to suggest 10-15% elongation.
(f) Cladding failure occurred in test.

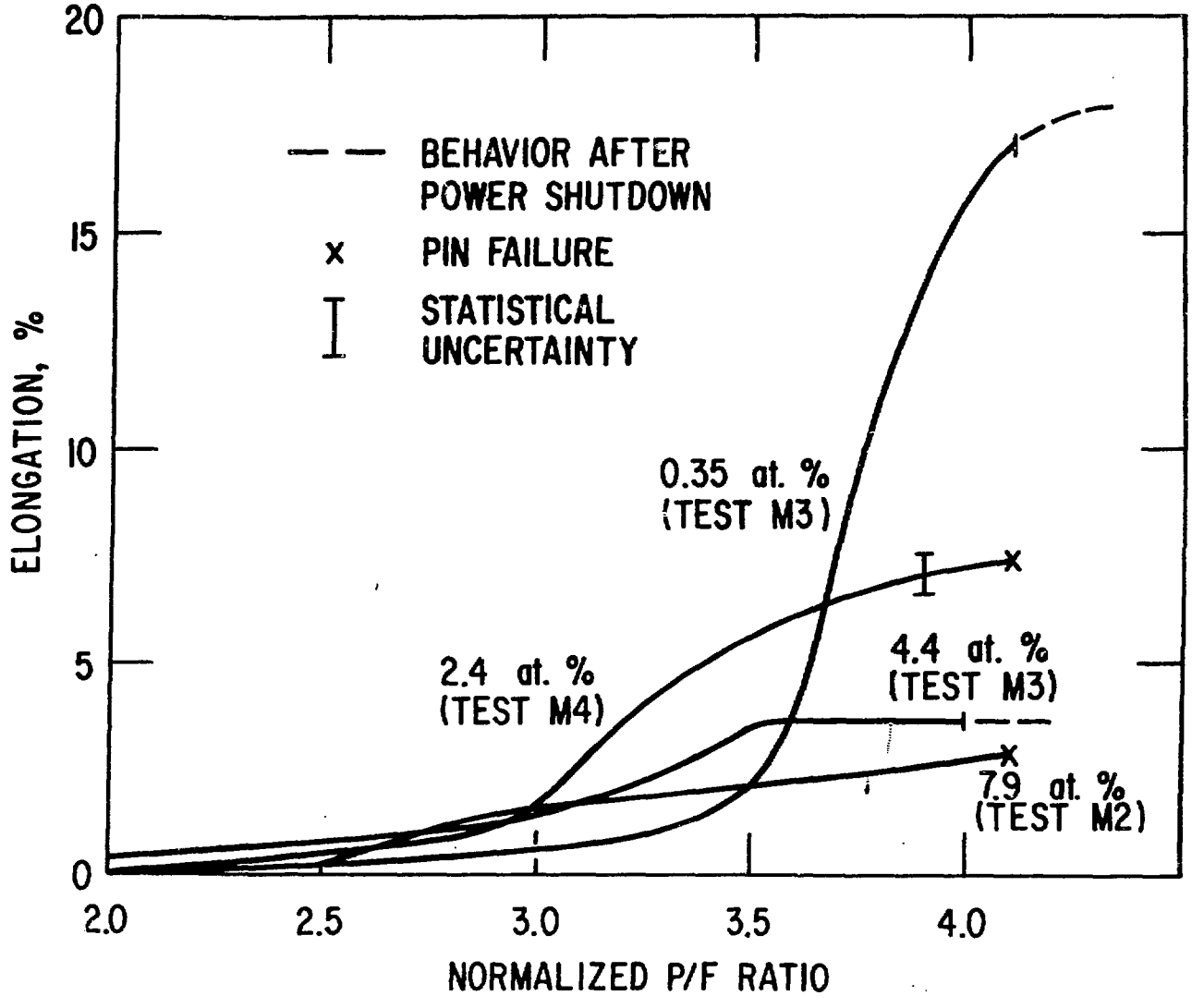
20
15
10
5
0
ELONGATION, %
BEHAVIOR AFTER POWER SHUTDOWN
PIN FAILURE
STATISTICAL UNCERTAINTY
0.35 at. % (TEST M3)
4.4 at. % (TEST M3)
2.4 at. % (TEST M4)
7.9 at. % (TEST M2)
2.0
2.5
3.0
3.5
4.0
NORMALIZED P/F RATIO

Figure 1.

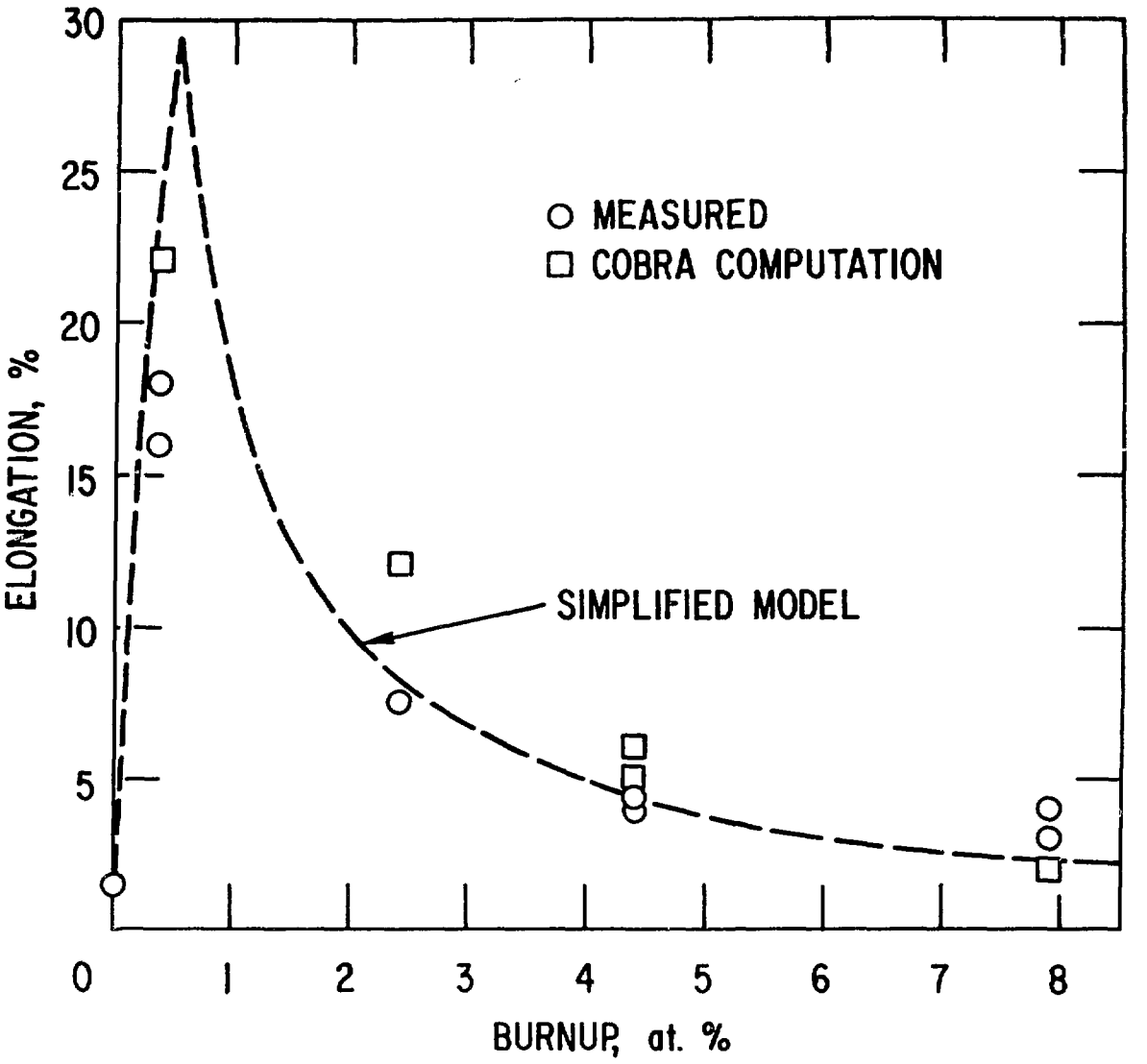
30
25
20
15
10
5
0
1
2
3
4
5
6
7
8
ELONGATION, %
BURNUP, at. %
MEASURED
COBRA COMPUTATION
SIMPLIFIED MODEL

Figure 2.

Figure 3.

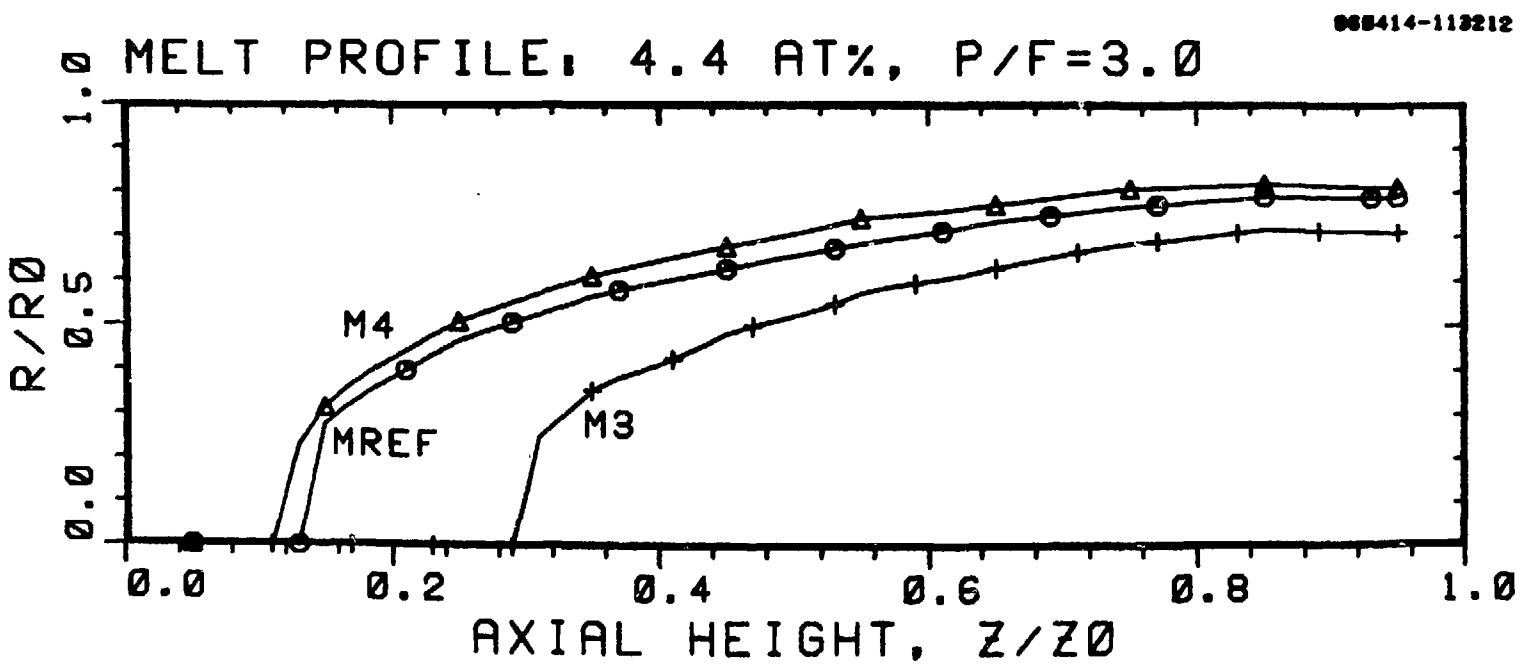
868414-113212
MELT PROFILE: 4.4 AT%, P/F=3.0
R/R0
1.0
0.5
0.0
M4
MREF
M3
0.0
0.2
0.4
0.6
0.8
1.0
AXIAL HEIGHT, Z/Z0